Geological Quarterly, 2010, **54** (4): 387–400

Sulphur and oxygen isotope signatures of late Permian Zechstein anhydrites, West Poland: seawater evolution and diagenetic constraints

Tadeusz Marek PERYT, Stanisław HAŁAS and Sofiya Petrivna HRYNIV

Peryt T. M., Hałas S. and Hryniv S. P. (2010) – Sulphur and oxygen isotope signatures of late Permian Zechstein anhydrites, West Poland: seawater evolution and diagenetic constraints. Geol. Quart., **54** (4): 387–400. Warszawa.

The stable oxygen and sulphur isotope ratios of 52 anhydrite samples from three Zechstein anhydrite units (Lower Anhydrite, Upper Anhydrite and Basal Anhydrite) of West Poland show δ^{f8}O values *vs*. VSMOW in the range of 9.4 to 15.5‰ (mean of 12.6 ±1.3‰), and δ^{34}S values *vs*. VCDT between 9.6 to 12.6‰ (mean of 11.4 ±0.6‰). A generally uniform distribution pattern of both isotopic values throughout the section, although with some random variation, implies that sulphate ions were sufficiently supplied and the basin was open during sulphate deposition. There is a slight stratigraphic differentiation of both the δ^{18}O and δ^{34}S values: the highest mean values are shown by the Upper Anhydrite and the lowest average values occur in the Basal Anhydrite. The correlation between δ^{18}O and δ^{34}S values is statistically significant only in case of the Basal Anhydrite. A wide range of oxygen isotopic ratios (from 11.6 to 25.1‰), with only several samples having δ^{18}O values that fall within the range of late Permian seawater, have been recorded in anhydrite cements and nodules that occur in the Main Dolomite rocks. Sulphur isotope ratios of anhydrite cements (range of 7.6 to 12.9‰, average of 10.7 ±1.4‰) tend to reflect the late Permian sulphur isotopic signature of sulphate in seawater. The higher ranges of δ^{18}O and δ^{34}S values of anhydrite cements and nodules in the Main Dolomite compared to the underlying and overlying anhydrites are due to diagenetic resetting. The conversion of gypsum to anhydrite (often very early and under negligible cover) evidently did not affect the primary marine stratigraphic sulphur isotope composition of the sulphate deposits.

Tadeusz M. Peryt, Polish Geological Institute – National Research Institute, Rakowiecka 4, PL-00-975 Warszawa, Poland, e-mail: tadeusz.peryt@pgi.gov.pl; Stanisław Hałas, Mass Spectrometry Laboratory, Institute of Physics, Maria Curie-Skłodowska University, PL-20-031 Lublin, Poland, e-mail: stanislaw.halas@poczta.umcs.lublin.pl; Sofiya P. Hryniv, Institute of Geology and Geochemistry of Combustible Minerals, National Academy of Sciences of Ukraine, Naukova 3A, 79060 Lviv, Ukraine, e-mail: sophia_hryniv@ukr.net
(received: September 8, 2009; accepted: August 25, 2010).

Key words: Permian, Zechstein, marine evaporites, sulphate isotopes, diagenetic isotopic resetting.

INTRODUCTION

The late Permian Zechstein Basin of NW and Central Europe is one of the classical giant evaporite basins (Fig. 1A). Evaporites that form the bulk of the basin fill originated through precipitation from marine-derived brines of sulphate-rich type which was characteristic of the parent, penecontemporaneous seawater, as indicated by the study of the compositions of fluid inclusions in sedimentary halite forms (Kovalevych *et al*., 2002). However, considering the palaeogeographic framework and especially a very limited and temporary connection with the ocean, the Zechstein Basin was in fact an intracontinental basin. Thus, it is reasonable to expect non-marine inputs not only during the terminal stages of the declining Zechstein evaporite basin but also during the early stages, related to the Werra and Stassfurt cyclothems (Fig. 2). A recent strontium isotope study indicated great consistency of results, characteristic of an ocean-based hypersaline water body, although some of the anhydrite beds at different brief periods, particularly at the marginal location, record an intermittent meteoric contribution to the ocean-based hypersaline water body (Denison and Peryt, 2009).

In addition to strontium isotopes, sulphur and oxygen isotopes are used to interpret depositional environments of marine sulphate deposits and to determine the parent fluids of the ancient evaporites. Besides being controlled by global cycles through geological time, they are controlled by local environmental factors (such as salinity increase, redox processes or non-marine contributions) and post-depositional alteration (e.g., Claypool *et al*., 1980; Pierre, 1989; Richardson and Hansen, 1991; Strauss, 1997). However, the primary marine stratigraphic sulphur isotope variation can be preserved in anhydrite despite significant burial and related diagenesis of an original gypsum deposit (Worden *et al*., 1997).

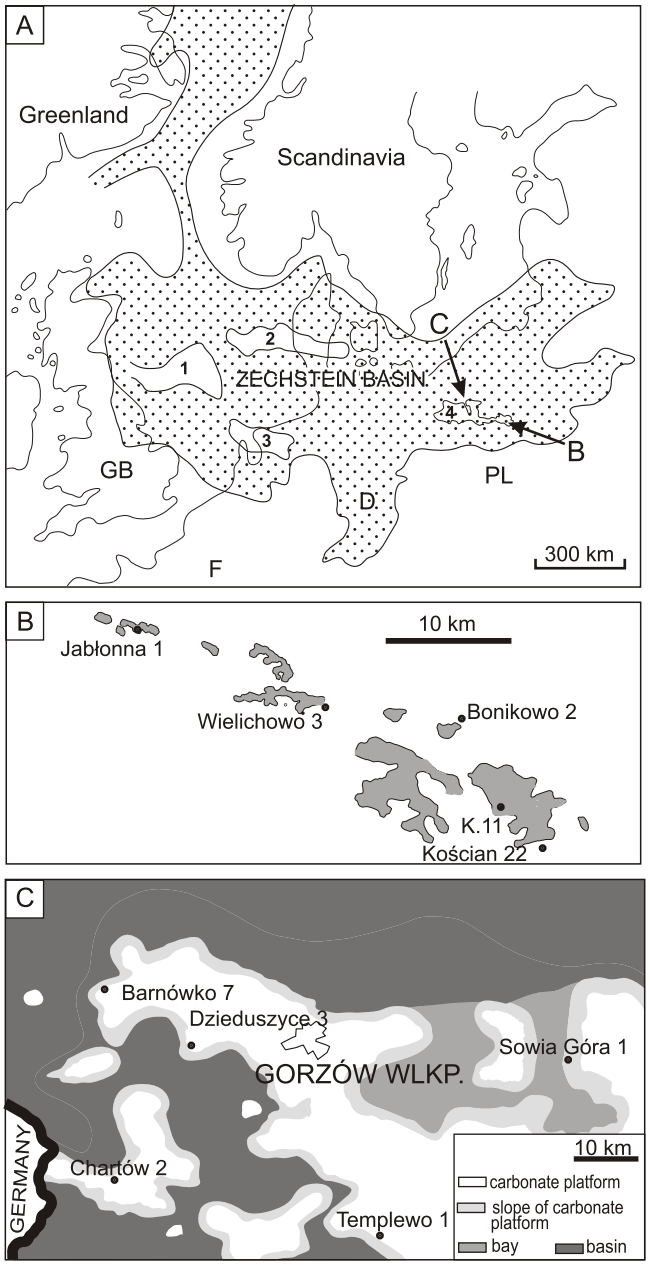

Fig. 1. Location map

A – the Zechstein Basin: 1 – Mid North Sea High, 2 – Ringkøbing-Fyn High, 3 – Texel High, 4 – Brandenburg–Wolsztyn–Pogorzela High; **B** – occurrence of reefs (grey) within the basinal facies (white) of the Zechstein Limestone in the Kościan area, West Poland (after Kiersnowski *et al*., 2010), showing the location of the boreholes studied; **C** – location of the boreholes studied in West Poland and the palaeogeography of the Main Dolomite (after Kovalevych *et al*., 2008, fig. 3, simplified)

This paper presents the results of study of sulphur and oxygen isotope ratios of 52 samples derived from the Zechstein anhydrites of the Werra and Stassfurt cyclothems in West Poland. These samples were collected from ten selected boreholes based on well-preserved cored sections and their various palaeogeographic locations (Fig. 1B, C). The earlier published data on the Werra and Stassfurt anhydrites are scarce (with the exception of North Poland). The reported $\delta^{34}S$ values for the Werra anhydrites of Germany (Nielsen and Ricke, 1964; Claypool *et al*., 1980; Kramm and Wedepohl, 1991; Kampschulte *et al*., 1998) vary from 10.5 to 12.6‰ (34 samples), whereas those of the Werra anhydrites (Lower Anhydrite and Upper Anhydrite) in North Poland are from 9.5 to 12.9‰ (31 samples). Eleven samples of the Stassfurt anhydrite from Germany have been studied so far (Nielsen and Ricke, 1964; Holser and Kaplan, 1966; Kramm and Wedepohl, 1991; Kampschulte *et al*., 1998) and they showed $\delta^{34}S$ values in the range of 10.1 to 11.8‰. The existing data set of the $\delta^{18}O$ values is limited to the Werra and consists of three $\delta^{18}O$ values (from 10.8 to 12.3‰) reported from Germany (Claypool *et al*., 1980) and 29 values (from 9.8 to 13.5‰) from Northern Poland (Peryt *et al*., 1998, 2005; Kovalevych *et al*., 2000; Hryniv and Peryt, 2003).

Only relatively few oxygen isotope determinations have been performed on sulphate evaporites, probably due to technical problems in making these measurements (Longinelli and Flora, 2007). Thus, the main aim of this work is: (1) to provide an additional set of oxygen isotope values for evaporite sulphates to the existing database to improve our knowledge of their variations through time, and (2) to distinguish between isotope ratios that represent primary solute sources and those that record syndepositional changes or subsequent diagenetic resetting.

GEOLOGICAL SETTING

The late Permian Polish Zechstein Basin is a part of the Southern Permian Basin that was initiated in the late Carboniferous. Several depressions separated by fault-bounded ridges occur within the Variscan orogen and its foredeep. One of these ridges is the Wolsztyn Ridge (part of the Variscan externides), which separated the Zielona Góra Basin from the Variscan Foreland. In the foreland and the Zielona Góra Basin, playa lake, eolian and wadi deposits up to 1000 m-thick accumulated during early Permian (Rotliegend) times, whereas Rotliegend deposits are absent from the Wolsztyn Ridge or are replaced by coeval volcanic rocks (Kiersnowski *et al*., 1995, 2010).

Deposition in the Polish Zechstein Basin commenced with flooding of the continental Rotliegend basin as a result of rifting-induced subsidence combined with a contemporaneous sea level rise (Peryt and Wagner, 1998). As a result of Zechstein Limestone deposition, a carbonate platform formed in marginal parts of the basin (Fig. 2) as well as on pre-Zechstein highs in the central part of the Wolsztyn Ridge, although in most cases reef bodies developed in these places (Dyjaczynski *et al*., 2001). The thickness of the reef complex reaches 90.5 m, and the deposition of the Zechstein Limestone resulted in a distinct enlargement of inherited relief. This relief was leveled by the deposition of the PZ1 evaporites, making the upper surface of the PZ1 (Werra) deposits roughly planar (Dyjaczynski *et al*., 2001; Figs. 2 and 3) because evaporite deposits are thin (*ca*. 25–40 m) in the reef zone and composed of the Upper Anhydrite only, whereas the evaporite sequence that encompasses the Lower Anhydrite, Oldest Halite and Upper Anhydrite is thicker (total thickness >100 m) outside the reef zone (Fig. 3).

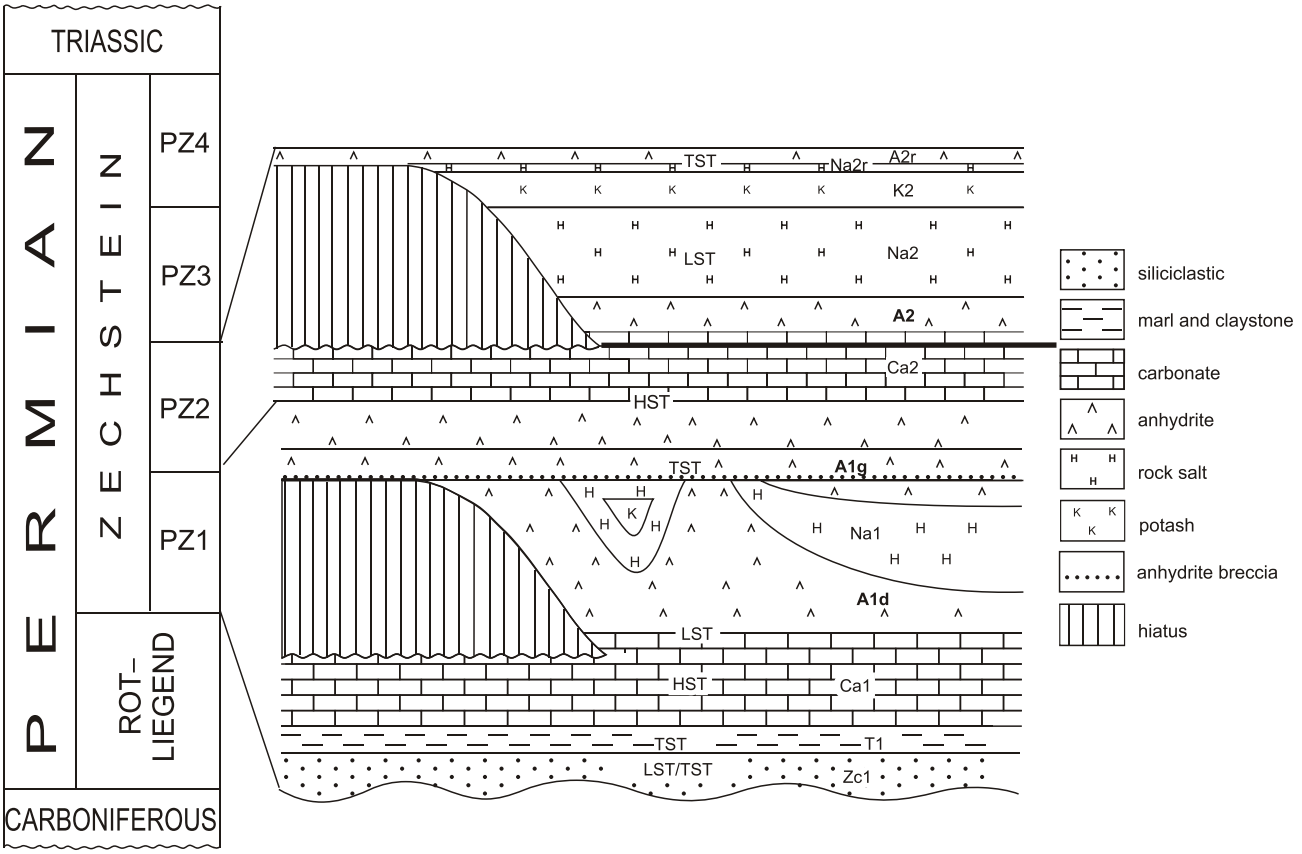

Fig. 2. Stratigraphy of the Zechstein PZ1 and PZ2 cycles in Poland

LST – lowstand systems tract, TST – transgressive systems tract, HST – highstand systems tract, after Peryt and Wagner (1998). Notice that the boundaries between HSTs and LSTs occur within the upper parts of carbonate units; Zc1 – Basal Conglomerate, T1 – Kupferschiefer, Ca1 – Zechstein Limestone, **A1d – Lower Anhydrite**, Na1 – Oldest Halite, **A1g – Upper Anhydrite**, Ca2 – Main Dolomite, **A2 – Basal Anhydrite**, Na2 – Older Halite, K2 – Older Potash, Na2r – Screening Older Halite, A2r – Screening Anhydrite. Anhydrite units studied are shown in bold

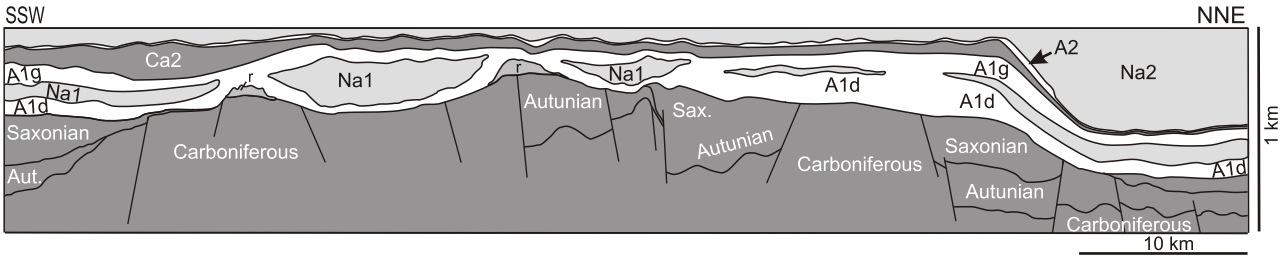

Fig. 3. Palaeogeological cross-section through the Wolsztyn High, along the NNE–SSW line, at the end of the Older Halite deposition (modified after Zielińska-Pikulska and Pikulski, 2002, unpubl.)

The cross-section is located outside Figure 1C and is passing through its lower right corner. Please notice that because of its negligible thickness the Zechstein Limestone is shown only in the reef area (r); anhydrite units are white; other explanations as in Figure 2

The subsequent depositional and burial history of the Wolsztyn Ridge was the same as that of the entire Fore-Sudetic Monocline that constituted a part of the Polish Basin. The PZ1 deposits (100 to 300 m thick) are covered by the younger Zechstein cycles: PZ2 (Stassfurt) (100 to >400 m thick), PZ3 (Leine) (100 to 200 m thick) and PZ4 (<100 m thick), and then by the Mesozoic (up to 3.5 km thick) and thin Cenozoic deposits. During late Permian and Mesozoic times, continual subsidence took place with periods of accelerated subsidence. At the end of the Jurassic, the Zechstein Limestone deposits were at a depth of *ca*. 3.5 km (Karnkowski, 1999, fig. 29), and the present base of the Zechstein Limestone lies at a 2.1–2.5 km depth. The present temperature at this depth is *ca*. 80°C (Karnkowski, 1999, fig. 42).

LITHOLOGY OF LOWER ANHYDRITE, UPPER ANHYDRITE AND BASAL ANHYDRITE

The Lower Anhydrite cores come mostly from the region in which Zechstein Limestone reefs developed (Fig. 1B). The lower part of the Lower Anhydrite shows a breccia appearance, then nodular anhydrite with clasts of red mudstones follows which is topped by selenitic anhydrite with upward-fining crystals. Eventually, nodular anhydrite that occurs at the base of the Lower Anhydrite gradually passes into anhydrite with pseudomorphs after upright-growth gypsum crystals, and higher anhydrite breccia and recrystallized clastic anhydrite with clear pseudomorphs after selenite crystals occur. In some cases clear fluidization was recorded within the bedded selenite which is characterized by small forms. The thickness of the Lower Anhydrite in the reef area is variable – the unit is thin (usually <30 m) or lacking above the reefs, but much thicker sections occur outside the proper reefs. In the borehole Bonikowo 2 the entire Lower Anhydrite is cored (Fig. 4), and in borehole Kościan 21 and Kościan 22 the core (58.6 and 67.3 m, respectively) comes from the lower part of the Lower Anhydrite. There occurs nodular, post-selenitic anhydrite with clear relics of bedding, and then bedded nodular anhydrite in borehole Bonikowo 2, in the lowermost part of the Lower Anhydrite (Fig. 4). In its upper part intercalations of massive brecciated, conglomeratic and recrystallized post-selenitic anhydrite occur, followed by mostly conglomeratic anhydrite and then bedded brecciated anhydrite with conglomeratic anhydrite interbeds, showing fluidization in the uppermost 1.5 m. In borehole Kościan 21, in the lower part of the core from the Lower Anhydrite, nodular anhydrite with dolomite streaks occurs, which is followed by recrystallized bedded anhydrite. In the upper part, bedded nodular anhydrite with streaks of dolomite and rare interbeddings enriched in clay material occurs; in the uppermost part fluidization was recorded. In borehole Kościan 22, in the lower part of the core nodular anhydrite (first bedded, next post-selenitic) occurs which is followed by recrystallized selenitic anhydrite with local fine clastic anhydrite interbeds in the lower part and post-selenitic nodular anhydrite in the upper part. Various parts (or even the entire section) of the Lower Anhydrite may show a nodular texture.

The Upper Werra Anhydrite is a few metres to over 250 metres thick in West Poland, but in the greater part of the peripheral part of the basin its thickness is a few tens of metres (Peryt *et al*., 1996*a*). In the area of the PZ1 sulphate platform, the Upper Anhydrite is usually (recrystallized) post-selenitic anhydrite with rare interbeds of clastic anhydrite (Fig. 4). Locally it is entirely clastic, or clastic in the bottom gradually passing into bedded selenitic anhydrite; it may exhibit slumping deformations. In borehole Bonikowo 2 anhydrite breccia at the bottom is replaced by nodular anhydrite with carbonate streaks (Fig. 4). In borehole Kościan 11 anhydrite breccia with a great amount of dolomitic matrix is replaced by nodular anhydrite, in places conglomeratic with interbeds, a few to tens of centimetres thick, of bedded anhydrite occur, and in the upper part recrystallized bedded anhydrite with more and more clear pseudomorphs after selenite crystals occurs (Fig. 4). In the basinal area, the Upper Anhydrite is laminated and shows graded bedding.

The Basal Anhydrite is usually a few to a dozen metres thick and, only in the area characterized by the occurrence of the up-

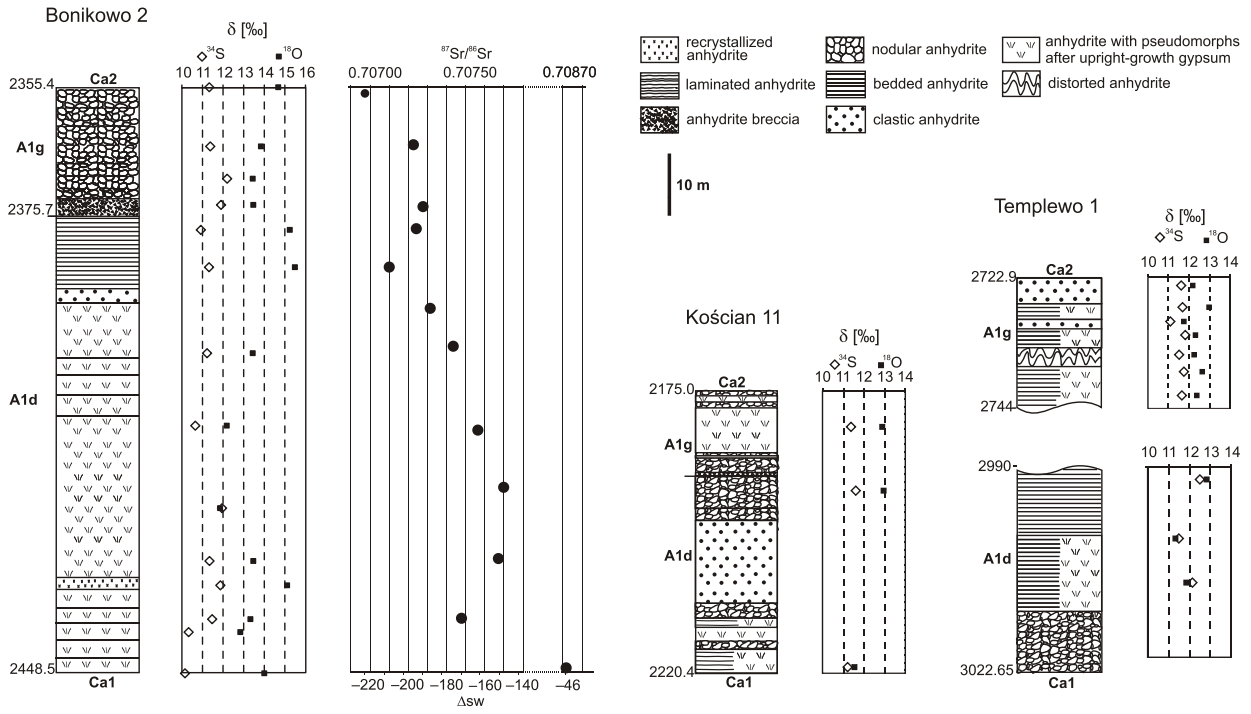

Fig. 4. Sections of PZ1 anhydrites of the Bonikowo 2, Kościan 11 and Templewo 1 boreholes, showing results of the oxygen, sulfur and, in the Bonikowo 2 section, strontium isotope measurements (the latter after Denison and Peryt, 2009)

Explanations as in Figure 2

permost slope of the Main Dolomite platform, its thickness reaches up to several tens of metres (Peryt *et al*., 1996*b*). The Basal Anhydrite begins with stromatolitic anhydrite (a few tens of centimetres thick) followed by bedded anhydrite with pseudomorphs after selenite crystals. The height of pseudomorphs varies from several millimetres to about ten centimetres; the highest pseudomorphs occur in the lower part of the Basal Anhydrite. The pores after selenite crystals are often filled with halite. In some cases there occurs clastic anhydrite with clasts originated from broken selenite crystals. The Basal Anhydrite contains halite intercalations (Peryt *et al*., 1996*b*). These intercalations are 1 cm to several metres thick (e.g., 2.65 m in borehole Chartów 2), and these thick halite intercalations contain anhydrite laminae which are several to 10 cm apart. They are followed by laminated anhydrite (with pseudomorphs after selenite crystals) with halite intercalations (10–30 cm thick in borehole Chartów 2; Kovalevych *et al*., 2008).

MATERIAL AND METHODS

We have selected ten boreholes from the area of the Wolsztyn High in which the studied sulphate horizons were cored either partly or entirely (Bonikowo 2 and Kościan 22); in most cases only portions adjacent to carbonate horizons were cored and thus available to study. The Lower Anhydrite was studied in six boreholes, the Upper Anhydrite in six boreholes, and the Basal Anhydrites in five of them (Table 1). The location of boreholes is shown in Figure 1. Selected samples were subjected to isotopic (S and O) study (52 samples). In two of the boreholes examined (Bonikowo 2 and Kościan 22) the strontium isotopic composition has been earlier established (Denison and Peryt, 2009); nine of the previously studied samples have been analysed for stable oxygen and sulphur isotopes.

The samples were powdered in an agate mortar, then *ca*. 100 mg of the powder was dissolved in distilled water acidified with HCl to pH = 1. The dissolution was performed in 250 mL glass beakers filled to *ca*. 1/3 of their volume. The beakers were covered by watch glasses, stored under a fume hood over several days and stirred several times a day. After dissolution of sulphates the solutes were filtered to small glass beakers and $BaSO_4$ was precipitated by means of an acidified (with HCl) solution of $BaCl_2$. The precipitate was washed by distilled water several times until the disappearance of chloride ions, which were tested in the remaining filtrate using 10% $AgNO_3$ solution. Clean $BaSO_4$ precipitates were dried in small breakers in an oven at 100°C and then subjected to the procedures for quantitative extraction of sulphur and oxygen for isotope analysis. Under the conditions described, no influence of isotope exchange between sulphate ions and water was observed due to low ambient temperatures (16 to 18°C) and the escape of a major fraction of HCl from the beakers to the atmosphere within a few hours.

The isotope ratios ($\delta^{34}S$ and $\delta^{18}O$) were determined by means of a dual inlet and triple collector mass spectrometer on SO_2 and CO_2 gases, respectively. SO_2 was extracted by the method developed in the Lublin laboratory (Halas and Szaran, 2001, 2004), whereas CO_2 was prepared by the method described by Mizutani (1971) and improved by Halas *et al.* (2007). We used typically 8 to 12 mg of $BaSO_4$ in each preparation; however, when necessary we were able to analyse 1 mg $BaSO_4$. The reproducibility of both analyses (2 standard deviations), obtained on the basis of replicated SO_2 extractions, was about 0.16‰. Delta values were normalized to the VCDT and the VSMOW scales by analysis of the NBS-127 standard, for which we accepted $\delta^{34}S$ = 21.14‰, after Halas and Szaran (2001), and $\delta^{18}O$ = 8.73‰ according to the recent calibration performed *vs*. VSMOW by Halas *et al*. (2007).

In addition, twelve samples of carbonate rocks with anhydrite nodules and cement that come from the Main Dolomite of four boreholes were analysed for S, C and O isotopes following the procedure described above, and besides, two samples of anhydrite nodules in the Main Dolomite were analysed for S and O isotopes. CO_2 was extracted from the carbonate samples using the selective chemical separation technique described by Al-Aasm *et al.* (1990). CO_2 was obtained at 25°C in 2 hours of reaction with 100% phosphoric acid for analysis of calcite. Then the sample kept on reacting until the next day and thereafter all CO_2 was pumped away. After that, the reaction was continued at 50°C over 2 days and CO_2 was collected for the isotopic analysis of dolomite. The isotopic analysis was performed on a dual inlet and triple collector mass spectrometer with standard uncertainty of $\delta^{13}C$ and $\delta^{18}O$ values of 0.07‰.

RESULTS

The oxygen and sulphur isotope analyses were determined on 52 anhydrite samples from the sulphate intervals (Tables 1 and 2; Fig. 5). The $\delta^{18}O$ values *vs*. VSMOW vary from 9.4 to 15.5‰ (mean of 12.6 ±1.3‰), whereas the $\delta^{34}S$ values *vs*. VCDT are in a narrower range of 9.6 to 12.6‰, with a mean of 11.4 ±0.6‰). The average $\delta^{34}S$ value for the anhydrites examined is thus close to that characteristic for the late Permian (10.9 ±1.3‰, according to Kampschulte and Strauss, 2004). The range (and average) $\delta^{18}O$ values obtained from this study differ from those (limited) values reported by Claypool *et al.* (1980) for the Zechstein anhydrites.

Taking into account the average gypsum-water ^{34}S fractionation of +1.65‰ (Thode and Monster, 1965), the original Zechstein brine would have had an average $\delta^{34}S$ value of about 9.25‰. In turn, considering the fractionation due to crystallization, $\delta^{18}O$ being 3.5‰ (Lloyd, 1968), the average original Zechstein brine would have had a $\delta^{18}O$ of 9.1‰, i.e. within the range of modern values (8.6 to 10.1‰; see Playà *et al*., 2007, p. 278).

There is a slight stratigraphic differentiation of both the $\delta^{18}O$ and $\delta^{34}S$ values: the highest average values occur in the Upper Anhydrite (13.1 ±0.9‰ and 11.7 ±0.35‰, respectively) and the lowest mean values occur in the Basal Anhydrite (10.9 ±0.7‰ and 10.9 ±0.6‰, respectively; Tables 1 and 2; Fig. 5). The Lower Anhydrite shows the greatest range of both the $\delta^{18}O$ and $\delta^{34}S$ values, the Upper Anhydrite is characterized by a much greater range of $\delta^{18}O$ values and small range of $\delta^{34}S$ values, and in the Basal Anhydrite the range of both δ values is the smallest (Table 1 and Fig. 5). Despite those differences between individual anhydrite units, no clear vertical trend is re-

Table 1

Provenance of anhydrite samples studied and their $\delta^{18}O$ and $\delta^{34}S$ values

No.	Borehole	Sample number	Depth [m]	$\delta^{18}O$ VSMOW [‰]	$\delta^{34}S$ VCDT [‰]	Unit	Sample description
1	Barnówko 7	9	3187.70	14.13	11.83	A1g	pseudomorphs after selenite crystals; fluidal
2		5	3190.70	15.14	11.41		pseudomorphs after selenite crystals; fluidal
3		2	3194.70	13.83	11.67		bedded, with pseudomorphs after selenite crystals
4	Bonikowo 2	46	2307.30	10.94	11.35	A2	bedded-laminated with pseudomorphs after mm selenite crystals
5		24	2355.65	14.68	11.33	A1g	nodular
6		19	2365.00	13.84	11.38		nodular
7		17	2370.10	13.44	12.2		nodular
8		15	2374.25	13.47	11.9		breccia
9		14	2378.20	15.24	10.92	A1d	massive, brecciated
10		12	2384.10	15.49	11.32		massive, brecciated
11		5	2397.70	13.44	11.22		poorly bedded with pseudomorphs after selenite crystals
12		40	2409.15	12.18	10.65		nodular with relics of pseudomorphs after selenite crystals
13		34	2422.20	11.86	11.95		nodular with relics of pseudomorphs after selenite crystals
14		31	2430.55	13.47	11.34		nodular with relics of pseudomorphs after selenite crystals
15		O2	2434.40	15.11	11.87		finely crystalline
16		30	2439.75	13.33	11.47		nodular bedded with pseudomorphs after selenite crystals
17		29	2441.80	12.84	10.33		nodular bedded with pseudomorphs after selenite crystals
18		27	2448.30	12.90	10.15		nodular poorly bedded with pseudomorphs after selenite crystals
19	Chartów 2	13	2716.00	10.6	11.06	A2	bedded-laminated with pseudomorphs after selenite crystals (mm – 2 cm high)
20		12	2722.00	11.17	10.7		laminated with pseudomorphs after mm selenite crystals
21		11	2725.50	12.02	10.71		laminated within halite intercalation
22		10	2730.50	10.5	10.82		nodular, fluidal
23	Dzieduszyce 3	12	3014.10	9.43	9.63	A2	flaser bedded
24		6	3031.10	10.46	10.17		laminated
25		2	3078.10	12.87	12.00	A1g	fluidal clastic
26		5	3080.50	12.51	11.35		fluidal bedded
27	Jabłonna 1	C2	2325.90	13.71	11.54	A1d	breccia
28		B	2332.00	12.89	10.89		finely nodular
29		A	2335.95	13.41	11.62		finely nodular
30	Kościan 11	33	2137.00	11.04	11.05	A2	bedded with pseudomorphs after selenite crystals
31		38	2139.80	11.56	11.49		bedded with pseudomorphs after selenite crystals
32		26	2181.00	12.89	11.39	A1g	bedded with pseudomorphs after selenite crystals
33		21	2191.10	12.94	11.60	A1d	nodular, fluidal
34		34	2219.00	11.53	11.21		bedded with mm pseudomorphs after selenite crystals
35	Kościan 22	38	2244.00	11.96	12.18	A1d	nodular with relics of pseudomorphs after selenite crystals
36		32	2264.10	11.45	11.94		massive with relics of pseudomorphs after selenite crystals
37		22	2294.75	13.01	12.08		bedded nodular
38	Sowia Góra 1	2	3259.50	12.74	11.80	A1g	laminated graded bedded
39		3	3261.85	13.22	12.60		laminated graded bedded
40	Templewo 1	26	2678.00	11.44	11.59	A2	bedded with mm pseudomorphs after selenite crystals
41		22	2724.30	12.18	11.63	A1g	clastic
42		21	2727.75	12.97	11.68		bedded with mm pseudomorphs after selenite crystals
43		20	2730.00	11.75	11.10		bedded with cm pseudomorphs after selenite crystals
44		18	2732.20	12.33	11.83		recrystallized bedded
45		15	2735.32	12.24	11.51		distorted
46		13	2737.95	12.65	11.75		distorted
47		12	2741.77	12.39	11.64		bedded with pseudomorphs after selenite crystals
48		9	2991.95	12.84	12.51	A1d	bedded with pseudomorphs after selenite crystals
49		6	3001.30	11.34	11.51		bedded with pseudomorphs after selenite crystals
50		4	3008.20	11.85	12.14		bedded with pseudomorphs after selenite crystals
51	Wielichowo 3	G1	2408.25	11.33	11.48	A1d	subhorizontal vein filled by light crystalline anhydrite
52		G2	2408.25	11.4	11.38		host rock of sample G1: bedded with up to 1.5 cm high pseudomorphs after selenite crystals

For explanations see Figure 2

Table 2

Summary of $\delta^{18}O$ and $\delta^{34}S$ values of Zechstein anhydrites in West Poland

	n	$\delta^{18}O$ VSMOW [‰]				
		mean	median	maximum	minimum	standard deviation
Total	52	12.6	12.7	15.6	9.4	1.3
Lower Anhydrite A1d	23	12.8	12.9	15.5	11.3	1.2
Upper Anhydrite A1g	19	13.1	12.9	15.1	11.8	0.9
Basal Anhydrite A2	10	10.9	11.0	12.0	9.4	0.7
$\delta^{34}S$ VCDT [‰]						
Total	52	11.4	11.5	12.6	9.6	0.6
Lower Anhydrite A1d	23	11.4	11.5	12.5	10.2	0.6
Upper Anhydrite A1g	19	11.7	11.7	12.6	11.1	0.4
Basal Anhydrite A2	10	10.9	10.9	11.6	9.6	0.6

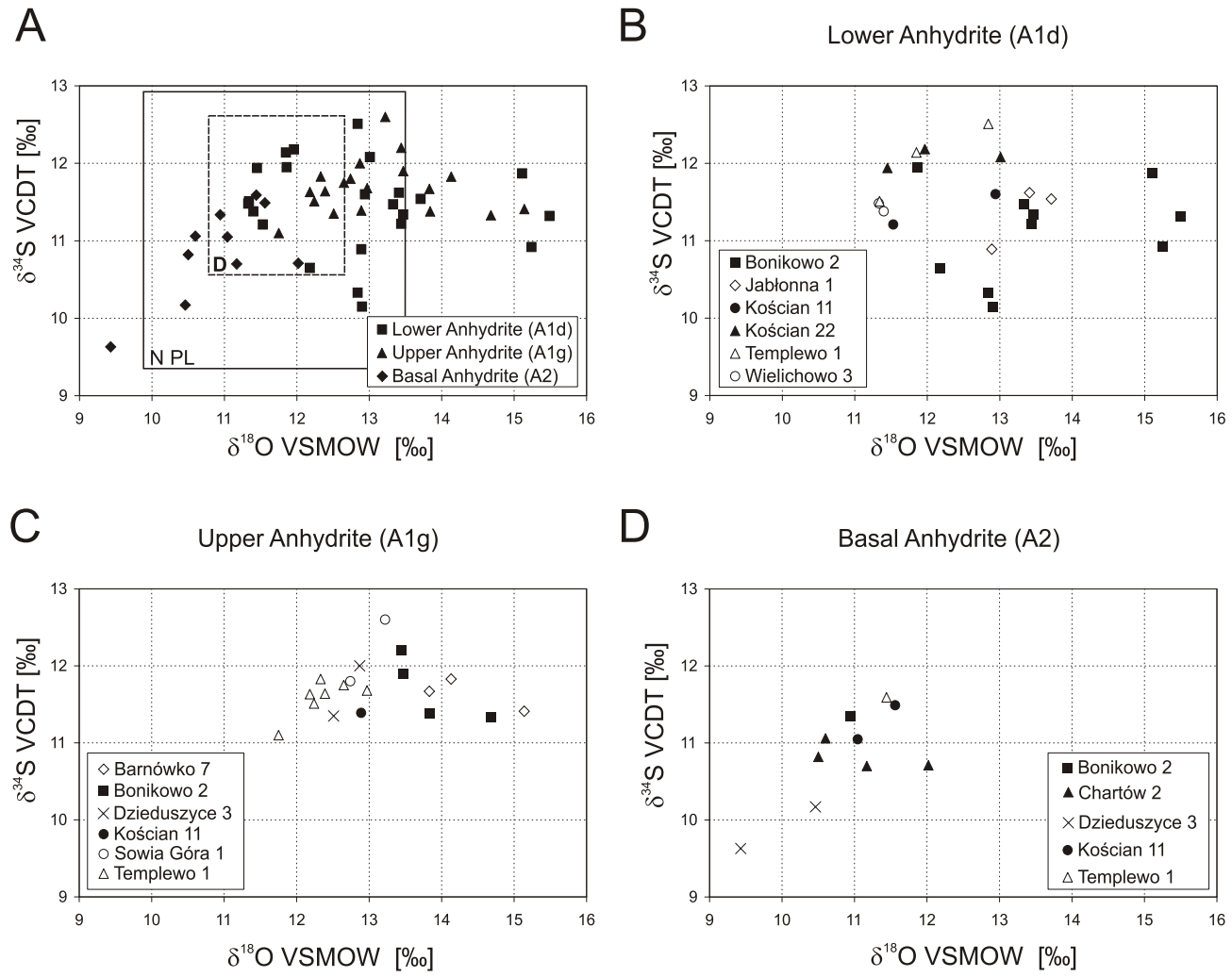

Fig. 5. Plots of isotopic data

A – all; **B** – Lower Anhydrite; **C** – Upper Anhydrite; **D** – Basal Anhydrite. The fields shown in A refer to the previous data reported in the literature for the Werra anhydrites of Germany (field D; after Nielsen and Ricke, 1964; Claypool *et al*., 1980; Kramm and Wedepohl, 1991; Kampschulte *et al*., 1998) and Northern Poland (field N PL; after Peryt *et al*., 1998, 2005; Kovalevych *et al*., 2000; Hryniv and Peryt, 2003)

Table 3

$\delta^{18}O$ and $\delta^{13}C$ values of Zechstein dolomites intercalated within anhydrites

Borehole	Depth [m]	Calcite		Dolomite	
		$\delta^{13}C_{VPDB}$	$\delta^{18}O_{VPDB}$	$\delta^{13}C_{VPDB}$	$\delta^{18}O_{VPDB}$
Jabłonna 1	2293.4	3.34	4.01	3.03	2.60
	2291.5	2.45	2.45	4.57	2.21
Jabłonna 2	2345.4	6.38	2.85	6.30	2.82
	2345.3	6.45	2.93	6.26	2.74
Jabłonna 3	2285.7	6.31	5.07	4.40	2.70
	2285.6	5.88	4.16	4.36	2.78
	2285.5	3.94	4.20	3.43	3.15
Wielichowo 3	2409.1	6.79	1.76	6.54	1.96
mean		5.2	3.4	4.9	2.6
standard deviation		1.7	1.1	1.4	0.4

corded. When plotted on a $\delta^{18}O$–$\delta^{34}S$ diagram, the slope of the regression line is –0.07 for the Lower Anhydrite, 0.01 for the Upper Anhydrite, and 0.58 for the Basal Anhydrite; when all the anhydrite units are plotted together, the slope of the relationship between $\delta^{18}O$ and $\delta^{34}S$ is 0.15.

The carbonate intercalations within the Lower Anhydrite show a range of $\delta^{18}O$ values *vs.* VPDB of 1.8 to 5.1‰ in calcite and 2.0 to 3.2‰ in dolomite (mean values of 3.4 ±1.1‰ and 2.6 ±0.4‰, respectively), and $\delta^{13}C$ values varying from 2.4 to 6.8‰ (mean of 5.2 ±1.7‰) in calcite and from 3.0 to 6.6‰ (mean of 4.9 ±1.4‰) in dolomite (Table 3 and Fig. 6). These values are different compared to those recorded in the Main Dolomite where the $\delta^{13}C$ values are more positive (mean values of 7.7 ±1.0‰ in calcite and 7.7 ±0.7‰ in dolomite) and the $\delta^{18}O$ values are more negative (mean values of 0.7 ±0.8‰ in calcite and 0.6 ±1.3‰ in dolomite; Fig. 7B; *cf.* Peryt and Scholle, 1996).

The mean $\delta^{18}O$ of anhydrite cements in the Main Dolomite deposits is 15.5 ±3.6‰. A wide range of $\delta^{18}O$ varying from 11.6 to 25.1‰, with only a few samples having $\delta^{18}O$ that fall within the range of late Permian seawater, have been recorded (Fig. 7A). The $\delta^{34}S$ values of anhydrite cements (mean of 10.7 ±1.4‰, range of 7.6 to 12.9‰; Fig. 7A) tend to reflect the late Permian sulphur isotope composition of seawater sulphate.

INTERPRETATION AND DISCUSSION

The obtained range of the $\delta^{34}S$ values in the Zechstein Werra anhydrites from West Poland is similar to that previously recorded for the Werra of Northern Poland (Peryt *et al.*, 1998, 2005; Fig. 5). Compared to the German Zechstein, the recorded ranges for the Lower Anhydrite and Basal Anhydrite in West Poland are slightly greater (*cf.* Nielsen and Ricke, 1964; Claypool *et al.*, 1980; Kampschulte *et al.*, 1998; Fig. 5). As far as the $\delta^{18}O$ values are concerned, their range in West Poland is larger than found so far in Germany and Poland (Nielsen and Ricke, 1964; Claypool *et al.*, 1980; Kampschulte *et al.*,

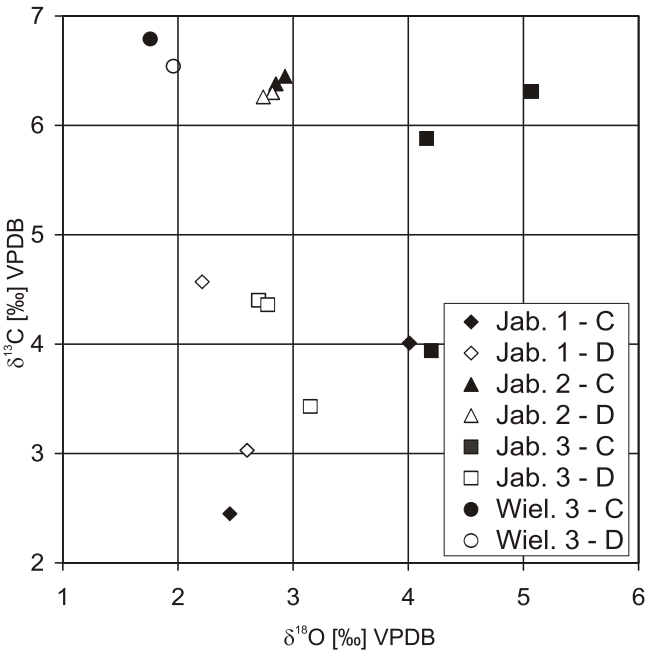

Fig. 6. Plot of isotopic data for carbonate intercalations within anhydrites

Jab. – Jabłonna, Wiel. – Wielichowo, C – calcite, D – dolomite

1998; Peryt *et al.*, 1998, 2005), and over one fifth of the samples studied from the Werra anhydrites show higher values, and one sample from the Basal Anhydrites shows a lower value than earlier reported for Poland (Fig. 5).

The normal marine range of sulphur isotope ratios in the Zechstein anhydrites indicates that the restriction of the basin was not complete. In addition, a relatively small deviation of the sulphur isotope ratios from that of late Permian seawater suggests that the anhydrites precipitated at relatively low temperatures because sulphur (and oxygen) is fractionated by chemical processes at elevated temperatures.

The major sources of sulphate to the marine sulphate reservoir are: (1) riverine sulphate, (2) sulphate from direct oxidation of sulphide and (3) sulphate from sulphur disproportionation reactions, and the $\delta^{18}O$ of soluble sulphate produced by disproportionation reactions in natural systems is likely to be in the range of 8 to 12‰ VSMOW (Bottrell and Newton, 2006). As the changes in the oxygen isotopic composition of marine sulphate are related to more complex processes than those affecting sulphur isotopes (see review by Bottrell and Newton, 2006), a fairly large variability of the $\delta^{18}O$ values can be expected, related not only to the changes in the bacterial sulphate reduction that largely affect the sulphur isotope values, but also to various oxidation processes that occur in buried sulphides.

The higher $\delta^{18}O$ and $\delta^{34}S$ values compared to those in the seawater indicate that continental contributions were not responsible for the high $\delta^{18}O$ and $\delta^{34}S$ values of the Zechstein anhydrites, and combined with the lack of upward decrease of $\delta^{18}O$ and $\delta^{34}S$ values in sections suggest that the reservoir effect played an insignificant role as regards variation in $\delta^{18}O$ and $\delta^{34}S$ of the Zechstein anhydrites. In turn, during deposition the sulphates probably underwent significant redox processes which account

Table 4

$\delta^{34}S$ and $\delta^{18}O$ values of anhydrite nodules and cements occurring in the Main Dolomite and their isotopic characteristics

No.	Borehole	Depth [m]	Host rock	Dolomite		Calcite		$\delta^{34}S$ VCDT [‰]	$\delta^{18}O$ VSMOW [‰]
				$\delta^{13}C$ VPDB [‰]	$\delta^{18}O$ VSMOW [‰]	$\delta^{13}C$ VPDB [‰]	$\delta^{18}O$ VSMOW [‰]		
1	Bonikowo 2	2327.2	dolomite: laminated mudstone	7.49	32.31			7.55	12.85
2		2339.0	recrystallized laminated dolomite	6.36	31.45	6.36	29.02	12.88	25.07
3	Dzieduszyce 3	3038.5	recrystallized dolomite	7.75	30.87			9.24	11.55
4		3040.25	recrystallized dolomite: peloidal-intraclast-biocl astic grainstone	8.09	31.24			10.81	14.81
5		3041.0	recrystallized dolomite: peloidal-intraclast-biocl astic grainstone	8.05	30.89			10.94	15.06
7		3050.0	recrystallized dolomite: peloidal grainstone	8.12	32.23			10.39	14.60
8		3062.35	dolomite: intraclast-peloidal wackestone-packstone	7.95	32.94			10.25	12.48
9	Kościan 11	2158.25	dolomite, mudstone	6.97	33.78			12.32	18.33
10		2164.8	recrystallized dolomite with bioclasts	7.02	33.18			12.41	16.86
11	Templewo 1	2692.2	dolomite, recrystallized grainstone	8.00	29.47	8.04	30.60	9.78	15.97
12		2705.0	dolomite, recrystallized grainstone	7.68	29.91	7.46	30.10	10.34	20.92
13		2711.25	dolomite, recrystallized grainstone	9.17	30.10	8.80	30.85	10.03	12.97
14	Sowia Góra 1	3250.25	dolomite, laminated mudstone					12.27	13.85
15		3256.25	dolomite, laminated mudstone					11.33	12.43

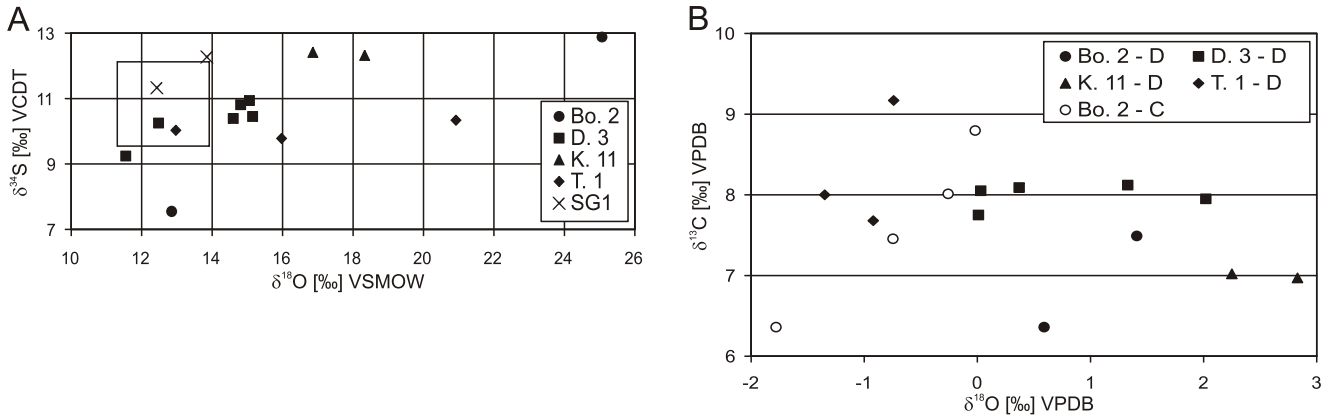

Fig. 7. Plots of isotopic data for the carbonates and anhydrite of the Main Dolomite

A – sulphates (box shows ranges of expected ratios if anhydrite was precipitated from late Permian seawater); **B** – carbonates; circles – Bonikowo 2 (Bo. 2), squares – Dzieduszyce 3 (D. 3), triangles – Kościan 11 (K. 11), diamonds – Templewo 1 (T. 1), X – Sowia Góra 1 (SG1); empty symbols are for calcite (C) and filled symbols are for dolomite (D)

for the deviation from normal marine ranges (*cf.* Lu *et al.*, 2001). The enrichment factor for $\delta^{18}O$ during a single stage sulphate reduction is around one quarter of that for $\delta^{34}S$ (Mizutani and Rafter, 1969) but repeated redox cycles of sulphate reduction produce higher $\delta^{18}O$ values (Bottrell and Raiswell, 2000). Modelling effects of redox cycling of sulphur during evaporite deposition on evaporite sulphate $\delta^{18}O$ yielded the maximum achievable shift in $\delta^{18}O$ (via long-term recycling in deep evaporating pans) of about 5‰ (Pierre, 1985; Lu *et al.*, 2001).

The correlation between $\delta^{18}O$ and $\delta^{34}S$ values is statistically important only in case of the Basal Anhydrite. The slope of the relationship (0.58) is slightly higher than that expected from the single effect of precipitation (0.47) (Thode and Monster, 1965; Lloyd, 1968). The lack of a gradual decrease upwards of the $\delta^{18}O$ and $\delta^{34}S$ values, which would be expected when the reservoir effect had taken place, and besides a rather uniform distribution of both isotopic values throughout the section, although with some random variation, implies that sulphate ions have been sufficiently supplied and that the basin was open during sulphate deposition.

The data on the late Permian Ochoan evaporites of the Delaware Basin (USA) show a smaller range and mean $\delta^{18}O$ values (8.4–12.2‰ and 9.6‰, respectively; Claypool *et al.*, 1980) and late Permian evaporites of Italy (Cortecci *et al.*, 1981; Newton *et al.*, 2004; Longinelli and Flora, 2007) show much higher $\delta^{18}O$ values (averaging 16.7‰ after Longinelli and Flora, 2007) compared to the Zechstein. The relatively narrow range (<3‰) of $\delta^{18}O$ values from Permian gypsum of Italy and their fairly regular distribution have been interpreted as due to rather homogeneous environmental conditions during the deposition of these evaporites despite the fairly large area of sample collection (Longinelli and Flora, 2007). Thus, the variability recorded in the Zechstein anhydrites studied indicates important changes of physico-chemical conditions during deposition in that part of the sedimentary basin. This conclusion is supported by the strontium isotope study of the Zechstein anhydrites in Poland, which indicated intermittent meteoric contributions to the ocean-based hypersaline water body (Denison and Peryt, 2009). Although the set of the Zechstein samples which were subjected to S, O and Sr isotopic analyses is rather limited, it is interesting to note that the deviations (either to more positive or more negative values of $\delta^{18}O$ and $\delta^{34}S$) fit the deviations of $^{87}Sr/^{86}Sr$ from the ideal late Permian marine signal (Fig. 8).

The anhydrite cements and nodules from the Main Dolomite often show greater ranges of $\delta^{18}O$ and $\delta^{34}S$ values compared to the underlying and overlying anhydrites (Fig. 7A). The most reasonable source of the sulphate forming nodules and cement in the Main Dolomite rocks is the bedded anhydrite deposits either above or below the Main Dolomite. In particular, it is commonly accepted that diagenetic anhydrite is commonly associated with reflux dolomites (Jones and Xiao, 2005). However, if the sulphate was derived directly from the bedded anhydrite, then the $\delta^{18}O$ and $\delta^{34}S$ of the anhydrite cement should reflect the late Permian seawater isotopic signatures. As this is not the case, then both the sulphur and the oxygen must have been fractionated during aqueous transport of the sulphate into the Main Dolomite (if the sulphate had originated from bedded anhydrite). Although low-temperature and high-temperature processes could result in such fractionations,

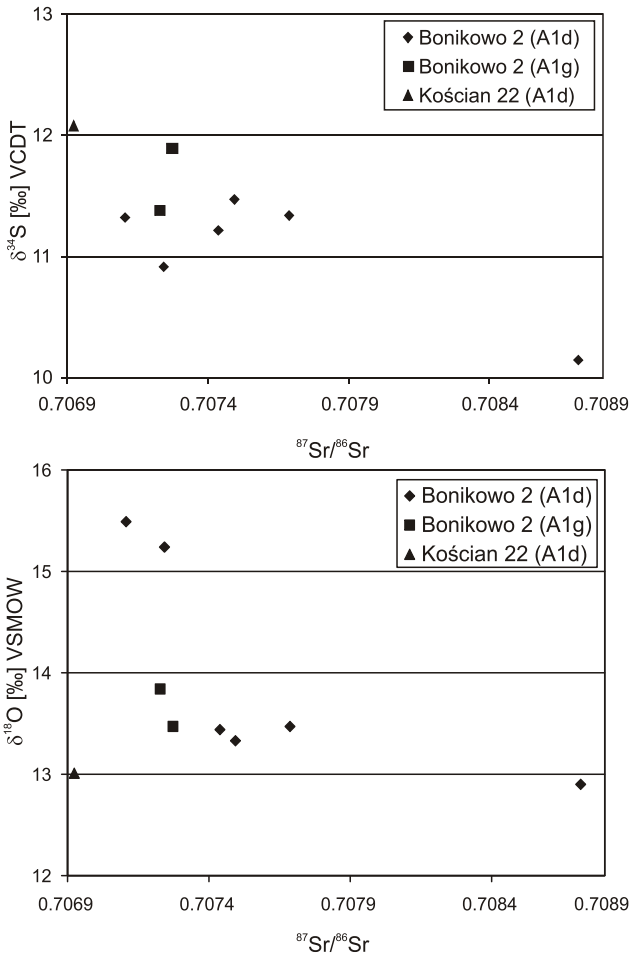

Fig. 8. $^{87}Sr/^{86}Sr$ (strontium isotope data after Denison and Peryt, 2009) of the PZ1 anhydrites *versus* $\delta^{18}O$ and $\delta^{34}S$ values

Other explanations as in Figure 2

the former cannot explain enrichment in the heavy sulphur isotope in the Zechstein anhydrites (see Dworkin and Land, 1994, for their discussion of the Louisiana basin case). In turn, the high-temperature process of thermally mediated sulphate reduction seems to be a plausible mechanism of the heavy sulphur isotope composition in the anhydrite cement. The most likely process responsible for the heavy isotope composition is thermal sulphate reduction and equilibration of sulphate oxygen with pore-fluid oxygen (see discussion by Dworkin and Land, 1994). Some samples of anhydrite cement in the Main Dolomite retain the seawater values while others underwent fractionation. This implies that either some of the sulphate was transported rapidly into the Main Dolomite before it had a chance to equilibrate fully or anhydrite cementation proceeded over a range of temperatures (*cf.* Dworkin and Land, 1994). Alonso-Azcárate *et al.* (2006) discussed an example of evaporites from Spain where Sr and sulphate-sulphur isotopic composition appears to represent the original composition of primary evaporitic gypsum, and evaporite sulphate $\delta^{18}O$ is enriched by about 10‰ relative to sulphate sources to the basin. This large effect resulted from re-equilibration of oxygen isotopes during low grade metamorphism when oxygen isotopes were open to exchange with aqueous fluids and/or interbedded

carbonates that constituted a large exchangeable oxygen reservoir (Alonso-Azcárate *et al.*, 2006). The maximum temperature which affected sulphate in the Zechstein anhydrite studied did not exceed 100°C, and the dolomite is enriched in ^{18}O (mean $\delta^{8}O$ of 31.5‰ compared to mean sulphate $\delta^{8}O$ of 15.9‰); thus, the enrichment of ^{18}O in sulphate has not been affected by isotopic equilibration with dolomite (*cf.* Alonso-Azcárate *et al.*, 2006). On the other hand, the oxygen isotopic enrichment in the sulphate could result at least partly from recycling, as clastic recycling is indicated by intercalations of clastic anhydrite, and this evidence suggests a possibility of accompanying chemical recycling.

The carbon and oxygen isotopic ratios of the Main Dolomite show clearly higher $\delta^{13}C$ values (by *ca*. 2.5‰) and lower $\delta^{8}O$ values (by *ca*. 3‰), combined with a greater spread of the latter (5‰) (Fig. 7B), compared to the carbonate intercalations in the Werra anhydrites where the spread of $\delta^{18}O$ values is <3.5‰ (Fig. 6). This is due to the strong association between the $\delta^{18}O$ data and palaeoenvironments in the Main Dolomite of Poland (Peryt and Scholle, 1996) and the origin of dolomite intercalations within anhydrite deposits in much stronger hypersaline settings compared to those in which the Main Dolomite sediments accumulated.

In most cases the original sulphate mineral was gypsum which underwent multistage dehydration. A considerable part of selenitic gypsum that formed sulphate platforms of the Lower Werra Anhydrite and Upper Werra Anhydrite was transformed into anhydrite at very early stages of diagenesis. The partial or complete replacement of gypsum by anhydrite is often very early: Hovorka (1992) indicated that a major part of such a replacement in the Permian of Palo Duro Basin occurred under a sediment cover less than 1 m-thick. Diagenesis in the presence of less-concentrated brines resulted in the obliteration of primary sedimentary structures due to the growth of nodules while the presence of highly-concentrated brines made it possible to preserve pseudomorphs after large gypsum crystals. In addition, the inflow of halite-saturated brines to the bottom of brine ponds caused a widespread replacement of gypsum by halite (Hovorka, 1992). Schreiber and Walker (1992) came to conclusion that the process of pseudomorphic replacement of gypsum by halite at the boundary of bedded sulphates and chlorides in cyclic evaporites is a feature of thermal non-equilibrium and hot brines – gypsum undersaturated and halite oversaturated – cause the replacement when they are in contact with the earlier originated gypsum substrate.

Some gypsum shows fluidal deformations, which could be a result of both gypsum dehydration that was due to the increasing pressure of overburden and temperature, as well as to the origin of gypsum diapirs. These diapirs have been recorded in the Zechstein of the Harz Mts. (Williams-Stroud and Paul, 1997). The gypsum is secondary, and the diapirs most probably were formed when the rock was primary gypsum, relatively early in the basin history. A very early origin of diapirs is indicated by the recorded deformations of unconsolidated Main Dolomite deposits. It is assumed that the origin of faults and laterally variable overburden pressure was of primary importance for the initiation of diapir growth (Williams-Stroud and Paul, 1997). In West Poland such deformations of the strata at the Upper Anhydrite–Main Dolomite boundary are fairly common, which can be related to the origin of such diapirs. On the other hand, a common local character (in places including a several-metre-thick bed) of fluidization occurrence suggests that the gypsum dehydration was due to the increasing pressure of overburden and temperature, and a sudden decline of fluidization indicates a complex pattern of circulation of dehydration solutions. In any case, it seems that the anhydritization of gypsum deposits occurred during the Zechstein deposition and in some cases it had a stepped nature. Therefore, it can be assumed that the origin of faults in the overburden of the Basal Anhydrite was related to the stages of intensive gypsum dehydration or the origin of gypsum diapirs.

IMPLICATIONS AND CONCLUSIONS

Most Zechstein anhydrites precipitated as gypsum (as indicated by common pseudomorphs after gypsum crystals) which underwent a multistage dehydration. The anhydritization of gypsum deposits occurred during the Zechstein deposition and often the partial or complete replacement of gypsum by anhydrite was very early and occurred under negligible cover. The conversion of gypsum to anhydrite did not evidently affect, as in the Permian–Triassic boundary interval in Abu Dhabi (Worden *et al*., 1997), the primary marine stratigraphic sulphur isotope composition. Worden *et al.* (1997) concluded that the primary differences in sulphur isotopes were preserved in the rocks and fluids and that significant mass transfer had not occurred: all reactions took place in situ and there was no significant sulphur isotope fractionation. We concur with that conclusion.

In contrast to the range of $\delta^{34}S$ values, which is within the range previously recorded from the Zechstein, the spread of $\delta^{18}O$ values is considerably larger in the Werra anhydrites of West Poland (Fig. 5A) due to a large variability of physico-chemical conditions during deposition of the Werra deposits in the part of sedimentary basin studied. At least a part of the recorded oxygen isotopic enrichment in the sulphate resulted from recycling, as clastic recycling is indicated by the common occurrence of clastic anhydrite, and this physical recycling could be coupled with chemical recycling. During the Stassfurt deposition the physico-chemical conditions became more stable.

Anhydrite cements and nodules in the Main Dolomite often show greater ranges of $\delta^{18}O$ and $\delta^{34}S$ values compared to those in the underlying Werra and overlying Stassfurt anhydrites (Fig. 7A), which served as the source for the sulphate that formed anhydrite nodules and cements. Because part of the samples with anhydrite cements in the Main Dolomite retain seawater values whereas the others underwent fractionation; either the sulphate was transported rapidly into the Main Dolomite before it had a chance to equilibrate fully, or anhydrite cementation proceeded over a range of temperatures (which can be neglected). Thus, although the syndepositional control was of primordial

importance, diagenetic resetting was an important factor that controlled the $\delta^{18}O$ values of Zechstein anhydrites.

Acknowledgements. The study was supported by the Polish State Committee on Scientific Research (Komitet Badań Naukowych; Grant No. 2 P04D 024 28) and the Polish Oil and Gas Company. We thank L. Antonowicz, A. Depowska, Z. Gregosiewicz and E. Iwasińska (POGC) and M. Jasionowski (Polish Geological Institute – National Research Institute) for their assistance throughout this study, A. Buniak and L. Pikulski for providing Figures 1C and 3, respectively, and Z. Migaszewski as well as the journal reviewers and A. Becker for comments and suggestions.

REFERENCES

AL-AASM I. S., TAYLOR B. E. and SOUTH B. (1990) – Stable isotope analysis of multiple carbonate samples using selective acid extraction. Chem. Geol., **80**: 119–125.

ALONSO-AZCÁRATE J., BOTTRELL S. H. and MAS J. R. (2006) – Synsedimentary versus metamorphic control of S, O and Sr isotopic compositions in gypsum evaporites from the Cameros Basin, Spain. Chem. Geol., **234**: 46–57.

BOTTRELL S. H. and NEWTON R. J. (2006) – Reconstruction of changes in global sulphur cycling from marine sulphate isotopes. Earth-Sci. Rev., **75**: 59–83.

BOTTRELL S. H. and RAISWELL R. (2000) – Sulphur isotopes and microbial sulphur cycling in sediments. In: Microbial Sediments (eds. R. E. Riding and S. M. Awramik): 96–104. Springer-Verlag. Berlin.

CLAYPOOL G. E., HOLSER W. T., KAPLAN I. R., SAKAI H. and ZAK I. (1980) – The age curves of sulfur and oxygen isotopes in marine sulfate and their mutual interpretation. Chem. Geol., **28**, 199–260.

CORTECCI G., REYES E., BERTI G. and CASATI P. (1981) – Sulfur and oxygen isotopes in Italian marine sulfates of Permian and Triassic ages. Chem. Geol., **34**: 65–79.

DENISON R. E. and PERYT T. M. (2009) – Strontium isotopes in the Zechstein anhydrites of Poland: evidence of varied meteoric contributions to marine brines. Geol. Quart., **53** (2): 159–166.

DWORKIN S. I. and LAND L. S. (1994) – Petrographic and geochemical constraints on the formation and diagenesis of anhydrite cements, Smackover sandstones, Gulf of Mexico. J. Sediment. Res., **A64**: 339–348.

DYJACZYNSKI K., GÓRSKI M., MAMCZUR S. and PERYT T. M. (2001) – Reefs in the basinal facies of the Zechstein Limestone (Upper Permian) of Western Poland. J. Petrol. Geol., **24**: 265–285.

HALAS S. and SZARAN J. (2001) – Improved thermal decomposition of sulfates to SO_2 and mass spectromeric determination of IAEA SO-5, IAEA SO-6 and NBS-127 sulfate standards. Rapid Comm. Mass Spectrom., **15**: 1618–1620.

HALAS S. and SZARAN J. (2004) – Use of Cu_2O–$NaPO_3$ mixtures for SO_2 extraction from $BaSO_4$ for sulphur isotope analysis. Isotopes Environ. Health Stud., **40**: 229–231.

HALAS S., SZARAN J., CZARNACKI M. and TANWEER A. (2007) – Refinements in $BaSO_4$ to CO_2 preparation and $\delta^{18}O$ calibration of the sulfate reference materials NBS-127, IAEA SO-5 and IAEA SO-6. Geostandards and Geoanal. Res., **31**: 61–68.

HOLSER W. T. and KAPLAN I. R. (1966) – Isotope geochemistry of sedimentary sulfates. Chem. Geol., **1**: 93–135.

HOVORKA S. (1992) – Halite pseudomorphs after gypsum in bedded anhydrite – clue to gypsum-anhydrite relationships. J. Sediment. Petrol., **62**: 1098–1111.

HRYNIV S. P. and PERYT T. M. (2003) – Sulfate cavity filling in the Lower Werra Anhydrite (Zechstein, Poland), Zdrada area, northern Poland: evidence for early diagenetic evaporite paleokarst formed under sedimentary cover. J. Sediment. Res., **73**: 451–461.

JONES G. D. and XIAO Y. (2005) – Dolomitization, anhydrite cementation, and porosity evolution in a reflux system: insights from reactive transport models. Am. Ass. Petrol. Geol. Bull., **89**: 577–601.

KAMPSCHULTE A., BUHL D. and STRAUSS H. (1998) – The sulfur and strontium isotopic compositions of Permian evaporites from the Zechstein basin, northern Germany. Geol. Rundsch., **87**: 192–199.

KAMPSCHULTE A. and STRAUSS H. (2004) – The sulfur isotopic evolution of Phanerozoic seawater based on the analysis of structurally substituted sulfate in carbonates. Chem. Geol., **204**: 255–286.

KARNKOWSKI P. H. (1999) – Origin and evolution of the Polish Rotliegend Basin. Pol. Geol. Inst. Spec. Pap., **3**.

KIERSNOWSKI H., PAUL J., PERYT T. M. and SMITH D. B. (1995) – Facies, paleogeography, and sedimentary history of the Southern Permian Basin in Europe. In: The Permian of Northern Pangea (eds. P. A. Scholle, T. M. Peryt and D. S. Ulmer-Scholle), **2**: 119–136. Springer, Berlin.

KIERSNOWSKI H., PERYT T. M., BUNIAK A. and MIKOŁAJEWSKI Z. (2010) – From the intra-desert ridges to the marine carbonate island chain: middle to late Permian (Upper Rotliegend-Lower Zechstein) of the Wolsztyn-Pogorzela High, West Poland. Geol. J., **45**: 319–335.

KOVALEVYCH V. M., CZAPOWSKI G., HAŁAS S. and PERYT T. M. (2000) – Chemiczna ewolucja solanek cechsztyńskich basenów ewaporatowych Polski: badania inkluzji fluidalnych w halicie z poziomów soli Na1–Na4. Prz. Geol., **48** (5): 448–454.

KOVALEVYCH V. M., PERYT T. M., CARMONA V., SYDOR D. V., VOVNYUK S. V. and HAŁAS S. (2002) – Evolution of Permian seawater: evidence from fluid inclusions in halite. Neues Jahrb. Miner. Abh., **178**: 27–62.

KOVALEVYCH V. M., PERYT T. M., SHANINA S. N., WIECŁAW D. and LYTVYNIUK S. F . (2008) – Geochemical aureoles around oil and- gas accumulations in the Zechstein (Upper Permian) of Poland: analysis of fluid inclusions in halite and bitumens in salt. J. Petrol. Geol., **31**: 245–262.

KRAMM U. and WEDEPOHL K. H. (1991) – The isotopic composition of strontium and sulfur in seawater of Late Permian (Zechstein) age. Chem. Geol., **90**: 253–262.

LLOYD R. M. (1968) – Oxygen isotope behavior in the sulphate water system. J. Geophys. Res., **73**: 6099–6110.

LONGINELLI A. and FLORA O. (2007) – Isotopic composition of gypsum samples of Permian and Triassic age from the north-eastern Italian Alps: palaeoenvironmental implications. Chem. Geol., **245**: 275–284.

LU F. H., MEYERS W. J. and SCHOONEN M. A. (2001) – S and O (SO_4) isotopes, simultaneous modelling, and environmental significance of the Nijar Messinian gypsum, Spain. Geochim. Cosmochim. Acta, **65**: 3081–3092.

MIZUTANI Y. (1971) – An improvement in the carbon reduction method for the isotopic analysis of sulfates. Geochem. J., **5**: 69–67.

MIZUTANI Y. and RAFTER T. A. (1969) – Oxygen isotopic composition of sulphates. Part 4. Bacterial fractionation of oxygen isotopes in the reduction of sulphate and in the oxidation of sulphur. N. Z. J. Sc., **12**: 60–66.

NEWTON R. J., PEVITT E. L., WIGNALL P. B. and BOTTRELL S. H. (2004) – Large shifts in the isotopic composition of seawater sulphate across the Permo-Triassic boundary in northern Italy. Earth Planet. Sc. Lett., **218**: 331–345.

NIELSEN H. and RICKE W. (1964) – Schwefel-Isotopenverhältnisse von Evaporiten aus Deuschland; Ein Beitrag zur Kenntnis von $\delta^{34}S$ im Meerwasser-Sulfat. Geochim. Cosmochim. Acta, **28**: 577–591.

PERYT T. M., KASPRZYK A. and ANTONOWICZ L. (1996*a*) – Upper Werra Anhydrite (Zechstein, Upper Permian) in Poland. Bull. Pol. Acad. Sc., Earth Sc., **44**: 121–130.

PERYT T. M., KASPRZYK A. and CZAPOWSKI G. (1996*b*) – Basal Anhydrite and Screening Anhydrite (Zechstein, Upper Permian) in Poland. Bull. Pol. Acad. Sc., Earth Sc., **44**: 131–140.

PERYT T. M., PIERRE C. and GRYNIV S. P. (1998) – Origin of polyhalite deposits in the Zechstein (Upper Permian) Zdrada platform (northern Poland). Sedimentology, **45**: 565–578.

PERYT T. M. and SCHOLLE P. A. (1996) – Regional setting and role of meteoric water in dolomite formation and diagenesis in an evaporite basin: studies in the Zechstein (Permian) deposits of Poland. Sedimentology, **43**: 1005–1023.

PERYT T. M., TOMASSI-MORAWIEC H., CZAPOWSKI G., GRINIV S. P., PUEYO J. J., EASTOE C. J. and VOVNYUK S. (2005) – Polyhalite occurrence in the Werra (Zechstein, Upper Permian) Peribaltic Basin of Poland and Russia: evaporite facies constraints. Carbonates and Evaporites, **20**: 182–194.

PERYT T. M. and WAGNER R. (1998) – Zechstein evaporite deposition in the Central European Basin: cycles and stratigraphic sequences. J. Seismic Explor., **7**: 201–218.

PIERRE C. (1985) – Isotopic evidence of the dynamic redox cycle of dissolved sulphur compounds between free and interstitial solutions in marine salt pans. Chem. Geol., **53**: 191–196.

PIERRE C. (1989) – Sedimentation and diagenesis in restricted marine basins. In: Handbook of Environmental Isotope Geochemistry. The marine environment (eds. P. Fritz and J. C. Fontes), **3**: 247–315. Elsevier, Amsterdam.

PLAYÀ E., CENDÓN D. I., TRAVÉ A., CHIVAS A. R. and GARCÍA A. (2007) – Non-marine evaporites with both inherited marine and continental signatures: the Gulf of Carpentaria, Australia, at ~70 ka. Sediment. Geol., **201**: 267–285.

RICHARDSON S. M. and HANSEN K. S. (1991) – Stable isotopes in the sulfate evaporites from southeastern Iowa, U.S.A.: indications of postdepositional change. Chem. Geol., **90**: 79–90.

SCHREIBER B. C. and WALKER D. (1992) – Halite pseudomorphs after gypsum: a suggested mechanism. J. Sediment. Petrol., **62**: 61–70.

STRAUSS H. (1997) – The isotopic composition of sedimentary sulfur through time. Palaeogeogr. Palaeoclimat. Palaeoecol., **132**: 97–118.

THODE H. G. and MONSTER J. (1965) – Sulfur-isotope geochemistry of petroleum, evaporites and ancient seas. Mem. Am. Ass. Petrol. Geol., **4**: 367–377.

WILLIAMS-STROUD S. C. and PAUL J. (1997) – Initiation and growth of gypsum piercement structures in the Zechstein Basin. J. Struct. Geol., **19**: 897–909.

WORDEN R. H., SMALLEY P. C. and FALLICK A. E. (1997) – Sulfur cycles in buried evaporites. Geology, **25**: 643–646.